Eur. Phys. J. B **24**, 395–403 (2001)
DOI:

THE EUROPEAN PHYSICAL JOURNAL B
EDP Sciences

Metastable structures of Dy layers adsorbed on Mo(112) and their transformations

A. Fedorus[1], V. Koval[1,†], A. Naumovets[1], and H. Pfnür[2,a]

[1] Institute of Physics, Natl. Academy of Sciences of Ukraine, Prospect Nauki 46, UA-03039, Kyiv-39, Ukraine
[2] Institut für Festkörperphysik, Universität Hannover, Appelstrasse 2, 30167 Hannover, Germany

Received 15 June 2001

Abstract. Ordering of dysprosium on Mo(112) up to 1.5 monolayers has been investigated by LEED and work function analysis after adsorption at 100 K and annealing between 200 and 1000 K. At low annealing temperatures (< 350–600 K) ordered structures are found, which are changed or even destroyed irreversibly by annealing steps to higher temperatures. At coverages, θ, up to 0.3 monolayer a (6×1) not strictly commensurate chain structure is seen, which coexists up to $\theta = 0.58$ with a one-dimensionally incommensurate c(1.56×2) structure. At higher coverages up to the physical monolayer at $\theta \approx 0.77$, incommensurate $(n \times 2)$ followed by oblique $(n \times 1)$ structures are seen with n continuously variable with coverage. The second layer forms a p(1.33×1) structure. Annealing to higher temperatures causes irreversible structural transitions with strongly coverage dependent properties. Up to $\theta = 0.58$, only a glass-like disordered phase is formed, which cannot be ordered again. In contrast, the rectangular incommensurate structures between $0.58 < \theta < 0.68$ remain unchanged upon annealing, whereas the structures at higher coverages and those of the second layer are transformed into commensurate $(s \times 1)$ structures with integer s. Geometrical models are presented for the non-annealed structures and possible origins for the two-dimensional concentration dependent vitrification of the Dy layers are discussed.

PACS. 68.55.-a Thin film structure and morphology – 64.70.Pf Glass transitions – 61.14.Hg Low-energy electron diffraction (LEED) and reflection high-energy electron diffraction (RHEED)

1 Introduction

The formation of linear-chain structures at low coverages with large distances between chains (up to 8 lattice constants) is a peculiarity of adsorption of atoms of many electropositive elements on channelled metal surfaces, such as the (112) faces of bcc crystals [1]. These have a similar structure as the (110) fcc surfaces. A particularly rich variety of the chain structures has been found for alkaline-earth but also for rare-earth adsorbates. This was attributed to the rather large electron density in their valence shells and the moderate dipole moments as compared to those for the alkali electropositive adsorbates. These features are believed to be responsible for a greater weight of the indirect interaction between the adatoms, *i.e.* the interaction mediated through the substrate electrons, relative to the dipole-dipole repulsion along the channels, so that the formation of the chain-like structures is favoured [1]. Contrary to the (110) surfaces of Au or Pt, on which superperiodicities are observed that differ from the bulk, the Mo(112) surface shows a (1×1) periodicity [2]. Only relaxations of the topmost layers, typical for open surfaces, have been found. The chain formation of the adsorbates mentioned above is not coupled with large reconstructions either, as revealed by LEED-IV structural analyses on the Li/Mo(112) [3] and Sr/Mo(112) [4] systems. From the adsorbate induced relaxations found in these studies, however, a subtle balance can be concluded between effective short range interactions that are responsible for the chain formation normal to the troughs of the substrate, and long range interactions due to Friedel oscillations of the charge density at the Fermi surface caused by the adsorbate induced redistribution of charge. For the latter mechanism to be effective with different sizes of unit cells, modifications of surface states must be involved.

However, some systems, namely Dy/Mo(112) and La/Mo(112) have been reported [1,5] to violate the mentioned regularity, *i.e.* no chain structures have been observed in spite of their rather small dipole moments (1.3 D and 1.8 D, respectively), whereas similar systems, characterized by even larger dipole moments, *e.g.* 3.6 D for Ba/Mo(112), obey the general trend. To investigate possible reasons of the above irregularity, we have undertaken a more detailed study of structure and work function changes in adlayers of dysprosium on the (112) surface

[a] e-mail: pfnuer@fkp.uni-hannover.de
[†] Deceased

of molybdenum. Contrary to the results just mentioned, we have found a chain-like structure at the early stage of Dy adlayer growth. This structure, however, turns out to be unstable against annealing. It is remarkable that most other ordered structures are also stable only at relatively low temperature. Upon high-temperature annealing, these actually metastable structures undergo irreversible transitions to more stable phases or to a glassy state. In this paper, we have investigated this interesting behaviour in detail. In Section 2 we describe the experimental conditions, the results are presented in Section 3 and their discussion in Section 4. Section 3 is split into two parts, one devoted to the low-temperature metastable phases, and another describing the annealing driven transitions.

2 Experimental

To perform the experiment, we used the UHV system and the experimental set-up described earlier [6–8]. Briefly, a SPECTALEED instrument equipped with a slow scan CCD camera was used for studying surface structure. The contact potential difference (CPD) method was used for monitoring work function changes. The stored images of the LEED patterns were used to obtain the peak intensities and full widths at half maximum (FWHM) for the particular spots. The same molybdenum specimen as in our previous works [7,8] was used as substrate, which is characterized by average (112) terrace sizes of 350 Å × 550 Å along the $[\bar{1}\bar{1}1]$ and $[1\bar{1}0]$ axes, respectively. An atomic-beam source of Dy was built in the form of a piece of dysprosium metal spot-welded to a tantalum ribbon serving as heater. A base pressure in the vacuum chamber between 0.7 and 1.5×10^{-11} mbar was kept all the time, *i.e.* both during dysprosium deposition and subsequent measurements. Auger electron spectroscopy was used to check purity of the substrate and adsorbate. The coverage θ is defined as the ratio of adsorbate to substrate surface atom concentrations. It was determined from the deposition time and from work function measurements calibrated by means of LEED in the coverage range $\theta = 0.68$–0.75. In this range of coverage the relation between coverage and LEED pattern is unique, since a single-phase incommensurate structure exists that undergoes uniaxial compression.

Deposition of the adsorbate was carried out at the lowest available substrate temperature (100 K) and the data were taken for the overlayers both as-deposited and after successive annealing to higher temperatures. Each annealing step lasted 10 s and was followed by a gradual temperature decrease at a rate of −5 K/s back to the base temperature. Most of the LEED observations were performed at an electron beam energy of 55–67 eV, *i.e.* close to intensity maxima of most superstructure spots.

3 Results

The structures described in the following sections have been annealed up to temperatures less than those at which annealing results in an irreversible structure transitions. The latter vary with coverage, and are specified below. Measurements have been taken usually at $T = 100$ K after annealing to T_a, unless specified otherwise.

3.1 Metastable low-temperature structures

The first extra features in the LEED patterns which are attributed to a (6×1) structure can be observed at a coverage of 0.07. They are readily seen for as-deposited films at the base temperature ($T = 100$ K). The location of the extra spots does not vary as a function of coverage up to $\theta = 0.3$, only their intensities gradually increase. This can be taken as evidence for growth of (6×1) islands. While annealing the film, some sharpening of the extra spots occurs up to an annealing temperature $T_a = 200$–250 K. Figure 1b shows the pattern of the best ordered structure (6×1). For this overlayer, *i.e.* close to a coverage of 0.3, the average domain size, estimated from the inverse half widths, goes up to 44 Å × 57 Å in $[\bar{1}\bar{1}1]$ and $[1\bar{1}0]$ directions, respectively. It is remarkable that some of the $^1/_6$-order spots show more anisotropy than others. This can be taken as an indication for a splitting that is not resolved with our instrument. This means that domain walls exist in the film already at coverages far below 0.33 so that the average periodicity along the $[\bar{1}\bar{1}1]$ direction is not exactly equal to six substrate spacings.

Variation of temperature within the above limits causes reversible changes in the peak intensity and full widths at half maximum (FWHM) of superstructure ($^1/_6$-order) spots. These are presented in Figure 2 for a coverage of 0.23. The temperature dependence of intensity shows a large Debye-Waller-like decrease already at low temperatures, typical of highly anisotropic floating solids [9]. No essential rise of FWHM is found in the range of reversibility despite of the significant decrease in intensity. Therefore, no order-disorder transition occurs. This means that the (6×1) phase at low temperatures shows the typical properties of an incommensurate two-dimensional solid, although the ratio of film-to-substrate spacing along the $[\bar{1}\bar{1}1]$ direction is very close to an integer number. Evidently, temperature is not low enough for pinning of the overlayer and its structure is not fully in registry with the substrate. A similar behavior was found recently for rarefied Sr overlayers on Mo(112) [8] at temperatures just above the depinning temperature.

Figure 3a shows a possible model of the (6×1) structure which is consistent with the LEED pattern and with the coverage at its maximum intensity. For simplicity, the model does not represent the small deviations of the adsorbate from the substrate registry perpendicular to the chains. Since two atoms per unit cell must be present according to our coverage calibrations, we suggest a two-level location of adatoms, *i.e.* the formation of a double-chain structure across the channels. Most chain-like structures reported earlier [1] (see also Refs. [3,4]) are formed by primitive $p(n \times 1)$ unit cells such as that formed by only one of the chains shown in Figure 3a. Although the distribution of atoms within the unit cell, based on our

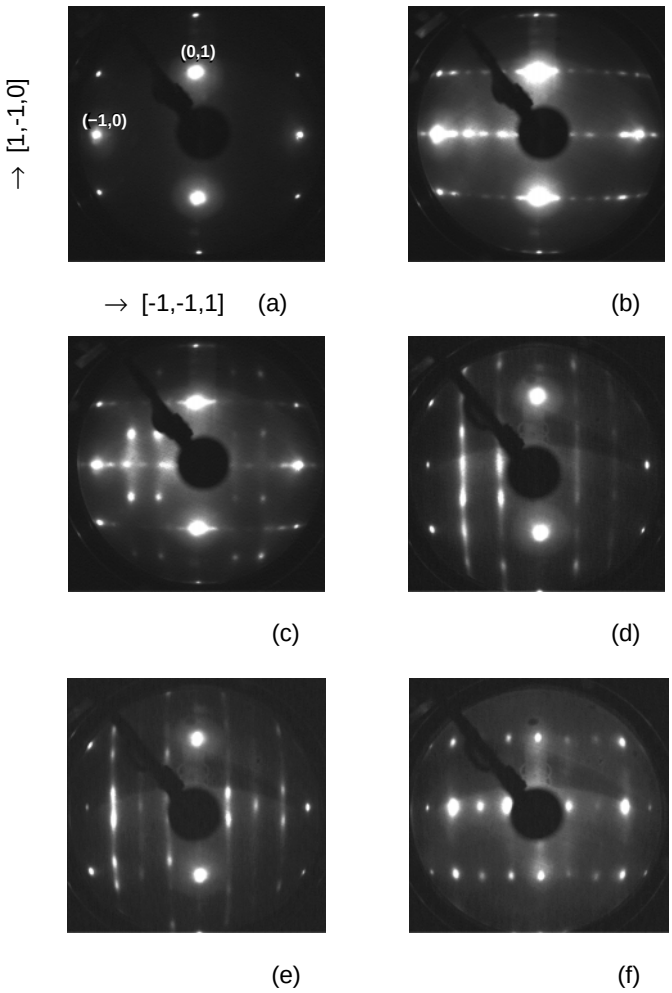

Fig. 1. LEED patterns from Dy/Mo(112) overlayers formed upon low-temperature annealing. Pattern from the clean substrate (a) is presented for a reference, with the principal axes and spots indicated. Coverage (monolayers): 0 (a); 0.25 (b); 0.46 (c); 0.68 (d); 0.74 (e); 1.4 (f). Annealing temperature (K): 200 (b); 400 (c); 800 (d); 500 (e); 200 (f). Electron energy (eV): 67 (a–c); 55 (d–f).

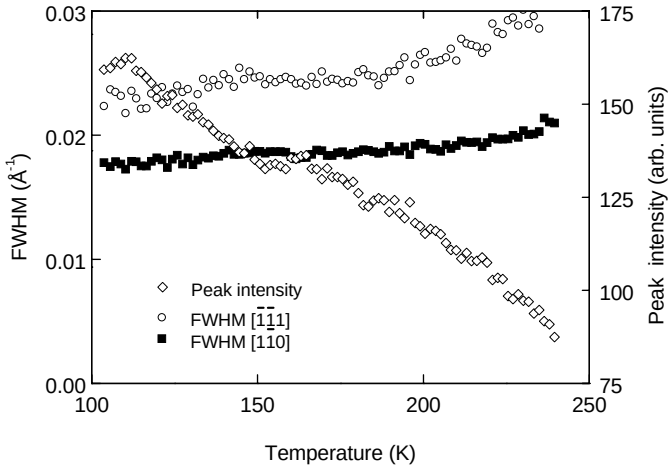

Fig. 2. Temperature dependence of the peak intensity of the $(-\frac{2}{3}, -1)$ LEED spot from the (6×1) structure and of its FWHM. $\theta = 0.23$.

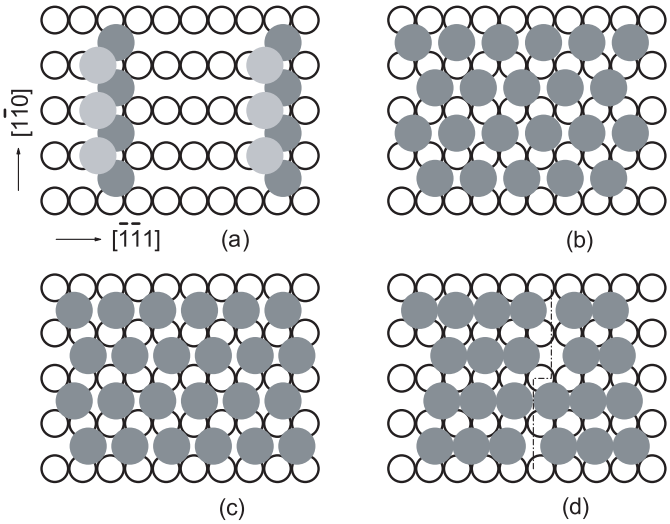

Fig. 3. Hard-sphere models for the ordered dysprosium overlayers: (6×1) (a); c(1.56×2) (b); (1.5×2) (c); (1.34×1) (d, domains of two mirror orientations are presented with the domain wall marked by a dash-dotted line). Light open circles show the topmost substrate layer, grey disks show the adsorbate layer. Darker balls correspond to increasing vertical depth. Principal axes are indicated.

experiments, is not unique, this model is motivated by the observation of a more complex chain, a zigzag chain, that was found for the (6×1) Ba/W(112) adlayer [10]. This diversity of chain formation indicates the complex nature of indirect interactions between adatoms which is responsible for chain formation [1,10]. A quantitative LEED-IV analysis would be able to resolve the remaining structural ambiguities.

Starting at $\theta = 0.3$, a new LEED structure, c(1.56×2) (see Fig. 1c), appears, which coexists with the (6×1) structure in the wide coverage range up to $\theta = 0.58$, *i.e.* a new phase grows *via* a first order phase transition. We note that the coverage value determined from the deposition time and that calculated from the lattice constants of the LEED pattern ($\theta = 0.64$) for maximum intensity of this structure still deviates by about 10%. It is concluded that ≈10% of the surface is still not covered by the c(1.56×2) phase, possibly due to a lack of full equilibration. Annealing results in better ordering of the c(1.56×2) structure in a limited range, below $T_a = 400$ K. It is clear that this c(1.56×2) structure is uniaxially incommensurate (see Fig. 3b), since an incommensurability between the adsorbate and substrate spacings, though small, was reliably recorded.

At coverages $\theta = 0.58$–0.68, the film undergoes uniaxial compression along the $[\bar{1}\bar{1}1]$ direction, keeping a rectangular $(n \times 2)$ lattice, in which n varies between 1.56 and 1.47. The unit cell must be non-primitive and contain two adatoms. However, in such a unit mesh, unlike that observed at lower coverages, the second adatom can not occupy a centre position. This is evident from the presence of some fractional order spots, namely $(-\frac{1}{\theta}, 0), (-\frac{1}{\theta}, -1), (-\frac{1}{\theta}, 1)$, which are clearly seen in

pattern d of Figure 1. These would be extinguished for centred structures. Figure 3c shows a possible real-space model that is consistent with the mentioned LEED features. It is worth noting that the (1.47×2) structure is absolutely stable and does *not* undergo an irreversible transition up to desorption temperatures.

The compression process causes an anisotropy of the correlation length. This is manifested in the LEED spot elongation that develops with increasing coverage (see Figs. 1d and e). It should be noted that upon compression of the $(n\times2)$ structure, an increase in anisotropy is coupled with an increase of the correlation lengths $(2R_c)$ along the substrate channel direction, $[\bar{1}\bar{1}1]$. Indeed, as estimated from the $(\mathrm{FWHM})^{-1}$ of the fractional-order spots in Figures 1c and d, the value of $2R_c$ remains practically constant across the channel ($\sim$30 Å), but increases as much as twice along the channel (from 41 to 84 Å).

The uniaxial compression continues with further increase of coverage until a uniaxially close-packed monolayer (at $\theta = 0.77$) is formed. In the coverage range between $0.7 < \theta < 0.77$ the unit cell $(n \times 1)$ is oblique, no longer rectangular. This is obvious from the LEED pattern shown in Figure 1e (note spot splitting in the $[1\bar{1}0]$ direction). Therefore, a coverage driven orientational phase transition has occurred. At first sight, this transition seems to be similar to that observed recently in the lithium overlayer on the same substrate at comparable coverages [7,11]. If the deviation from the rectangular cell sets in continuously as a function of coverage, this is characteristic for an instability of the shear modulus, *i.e.* rows of adatoms in adjacent troughs of the substrate can be (almost) freely shifted against each other at the critical coverage [7]. Theoretical treatment of this orientational phase transition (OT) predicts [12] that the shear modulus μ and the deviation of the angle α between the axes of the unit cell from 90° must change near the critical coverage θ_0 as $\mu \propto |\theta - \theta_0|$ and $\alpha \propto \sqrt{|\theta - \theta_0|}$. Hence a vanishing $[1\bar{1}0]$ component of the correlation length, R_c, is expected in the region of OT. This is not the case here, as seen from Figure 4, which shows the coverage dependences of the halfwidths and the inclination angle. No sign of a vanishing R_c in $[1\bar{1}0]$ direction was found in the vicinity of $\theta_0 = 0.68$, which separates the regions of existence of rectangular and oblique lattices. Although the steps of adsorbate deposition used in our experiment were small $(\Delta\theta = 0.03)$, it cannot be ruled out that the region of vanishing R_c was missed, but it is more likely that the orientational transition close to a coverage of 0.7 is of first order, and has a very narrow coverage range of coexistence. This type of transitions has been found before both in experiments [13,14] and in theory [15,16]. The decrease of α as a function of coverage above $\theta = 0.7$, on the other hand, suggests that, similar to the Li/Mo(112) system [7], there may be a second critical coverage close to $\theta = 0.85$ where a continuous transition back to the rectangular unit cell would occur. Both the continuous increase of FWHM as a function of coverage and a decrease of α, which is compatible with a square root law and a critical coverage of 0.85, point in this direction. Unfortunately, an increase of coverage beyond $\theta = 0.77$ results in formation of the second adsorbate layer so that this critical coverage cannot be reached. The oblique structures are stable up to $T_a \approx 550$ K.

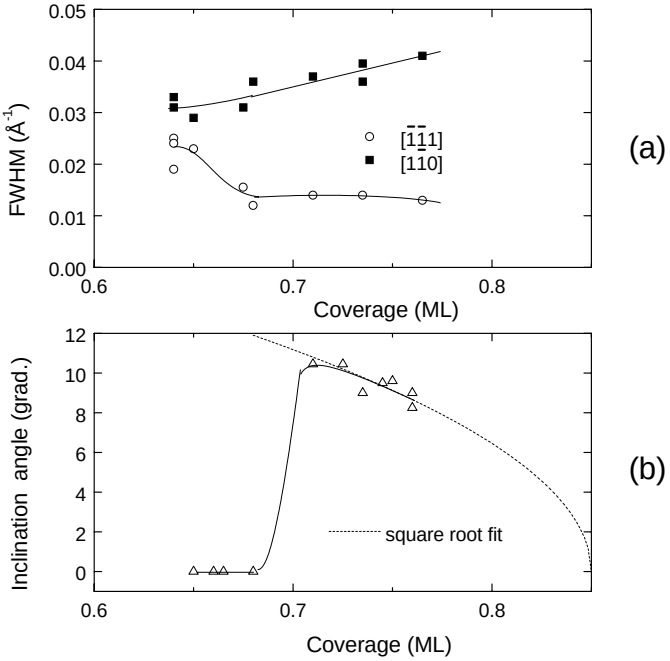

Fig. 4. Coverage dependence of FWHM of LEED superstructure spots (upper panel) and of the inclination angle (lower panel) of the unit cell in the region of the orientational transition. $T = 100$ K, $T_a = 500$ K.

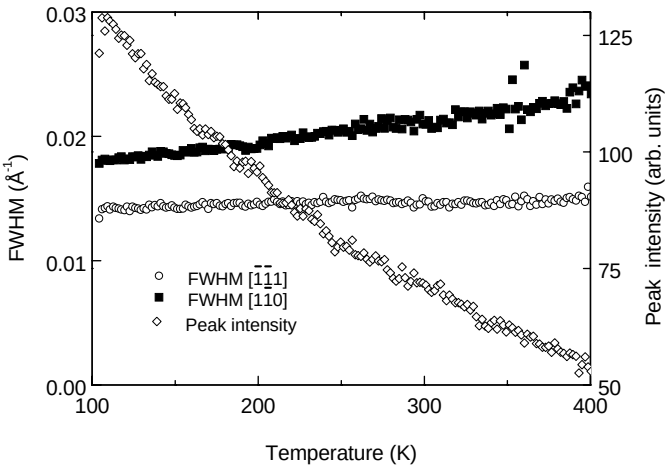

Fig. 5. Temperature dependence of the peak intensity of the $(-0.78, -0.82)$ LEED spot from the oblique structure ($\theta = 0.78$) and of its FWHM.

Both compressed structures, rectangular and oblique, are floating solids. This can clearly be seen from Figure 5, which shows temperature dependences of the LEED intensities and FWHMs. They reveal typical properties of uniaxial incommensurate two-dimensional crystals: the protracted intensity decay and the continuous increase of the halfwidths [9].

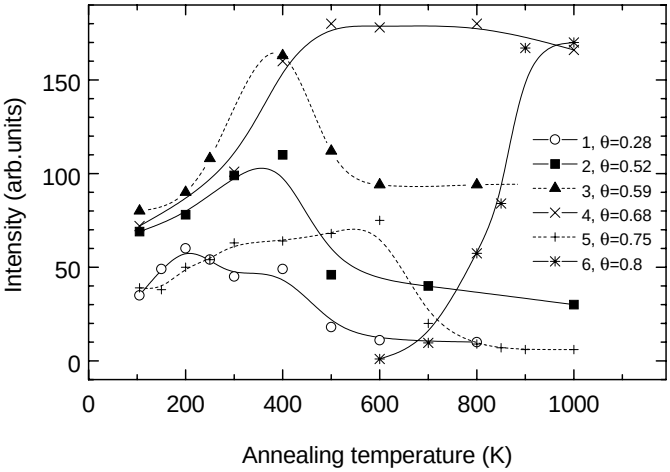

Fig. 6. Annealing-driven changes in intensity of fractional-order LEED beams for different structures of the Dy overlayer: $(6\times1)(1)$, c$(1.56\times2)(2)$, c(1.55×2) (3), rectangular (1.47×2) (4), oblique (1.3×1) (5), (5×1) (6). The beam intensity after annealing is always measured at $T = 100$ K.

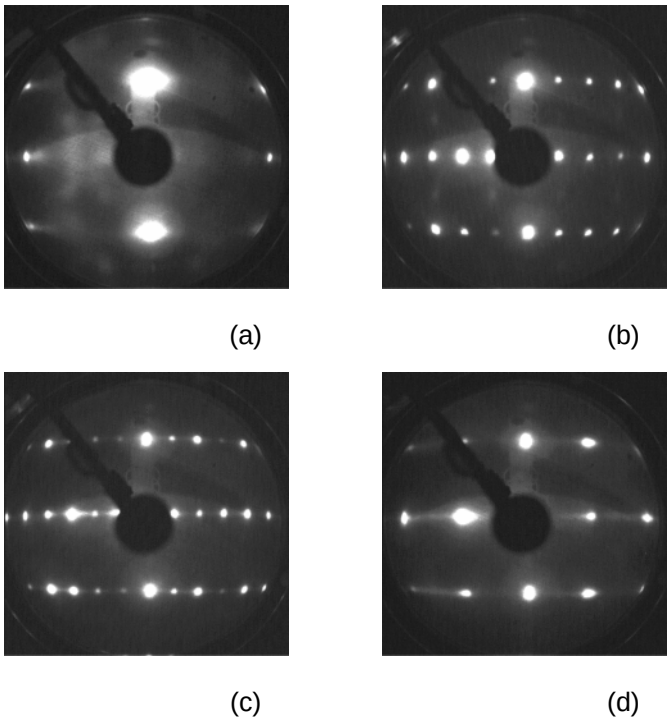

Fig. 7. LEED patterns from Dy/Mo(112) overlayers formed after high-temperature annealing. The patterns are recorded at $T = 100$ K. Coverage (monolayers): 0.45 (a); 0.735 (b); 0.8 (c); 1.04 (d). Annealing temperature (K): 800 (a); 1000 (b, c); 900 (d). Electron energy: 55 eV.

The second layer deposited onto the close-packed first monolayer forms a p(1.33×1) structure (Fig. 1f). The mode of growth of the second layer seems to keep a quasi-two-dimensional character only at low temperature (below $T_a \approx 200$ K) due to a limited mobility of the adsorbate. The p(1.33×1) structure is evidently stable against annealing up to $T_a = 500$ K. However, the intensity of its LEED spots decreases and the pattern of the underlying first monolayer appears. This indicates that coagulation in the second layer occurs (formation of thicker islands which occupy a smaller area). Evaporation of the second layer, which also could result in a similar effect, can be ruled out at these temperatures. Appreciable sublimation of Dy is expected only at temperatures above 1000 K.

3.2 Annealing driven structure transitions

Low-temperature annealing steps always resulted in improvement of the overlayer order for any Dy coverages above $\theta = 0.07$. As a measure of the degree of order, we use the peak intensity of LEED. Figure 6 shows a gradual initial gain in intensity of fractional-order beams for all coverages. However, at some coverages already annealing temperatures above 350 K are sufficient to trigger irreversible changes in the Dy adlayers.

At $\theta < 0.58$, the annealing effect is particularly unusual: a limited improvement of order for annealing temperatures up to $T_a \approx 400$ K is followed by an irreversible deterioration of the previous order without transition to any other ordered phase. This peculiarity is illustrated qualitatively by the disappearance of the fractional-order LEED spots in pattern (a) of Figure 7 and more quantitatively by intensity curves with local maxima followed by virtual fading of intensity (see Fig. 6). In the coverage region $\theta = 0.58$–0.6, order is only partially lost upon high-temperature annealing, but this effect is again irreversible, as shown by the intensity curve for $\theta = 0.59$ in Figure 6 which goes through a maximum and levels off at some intermediate intensity. In the following, we call "low annealing temperatures (LT)" those at which annealing results only in improvement of order in a metastable structure of the as-deposited film, whereas at "high annealing temperatures (HT)" annealing drives an irreversible structure transition.

Above $\theta = 0.58$, annealing results in the "usual" effect of steady improvement of order. This is illustrated for $\theta = 0.68$ in Figure 6: the intensity of fractional-order beams gradually increases and then levels off without any anomalies. The relevant LEED pattern from the annealed overlayer is shown in Figure 1d. In this particular case, there is no difference between LT and HT annealing. It should be noted that the lattice keeps its original symmetry upon annealing only in the narrow coverage range $\theta = 0.58$–0.68.

Films with coverages close to and above one physical monolayer $(0.68 < \theta < 1)$ also turn out to be unstable against annealing above 600 K. For coverages close to $\theta \approx 0.75$, they undergo irreversible transitions from the incommensurate oblique structure to a commensurate (4×1), whereas at θ equal to 0.8 and 1, (5×1) and (2×1) structures appear, respectively (see Figs. 7b–d). The corresponding pair of intensity curves is presented in Figure 6 for $\theta = 0.8$. Whereas the (4×1) LEED pattern can be interpreted as a "single-level" p(1.33×1) structure, the two latter patterns require a more complicated

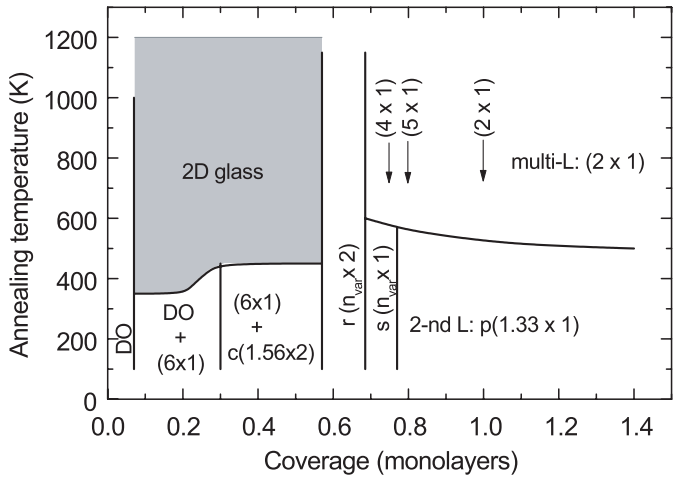

Fig. 8. Diagram of annealing-driven changes in structure of Dy overlayer on Mo(112). DO: disordered phase; 2D glass: two-dimensional glass (shadowed area); r($n_{\rm var}\times 2$) and s($n_{\rm var}\times 1$): rectangular and skew-angle structures, respectively, with a lattice spacing continuously varying with θ; 2nd L: second layer; multi-L: multi-layer structure. Arrows show the coverages at which the specified structures form.

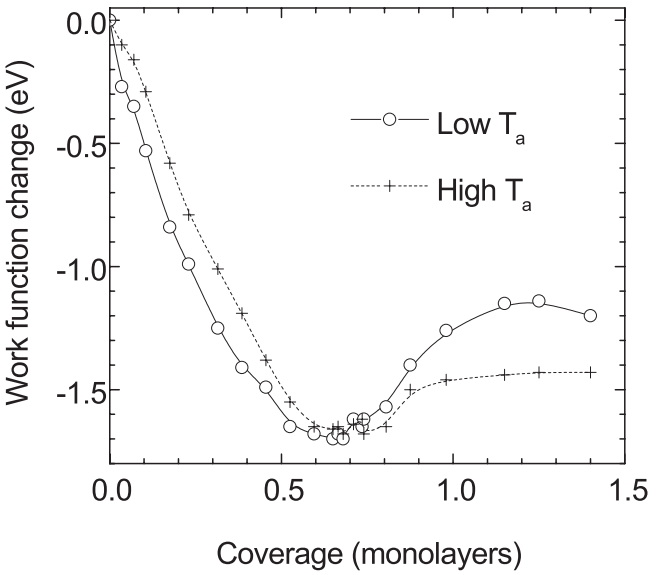

Fig. 9. Coverage dependence of the work function changes obtained after LT and HT annealing. Work function is measured at $T = 100$ K.

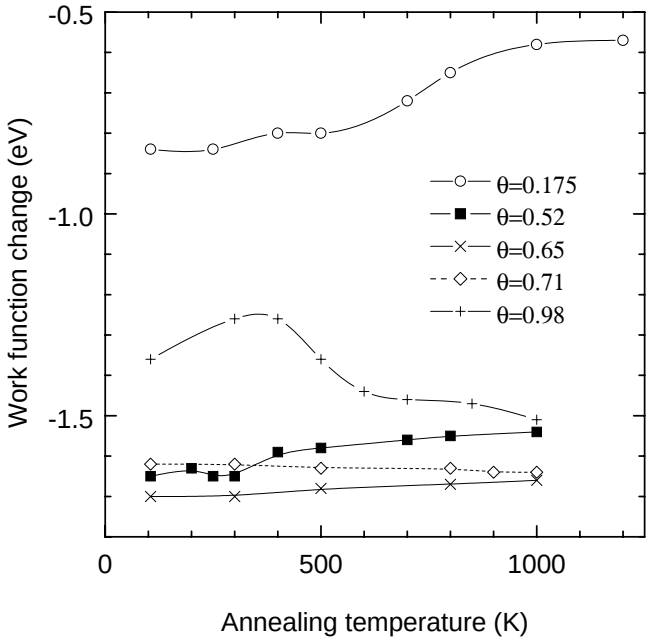

Fig. 10. Annealing effect on the work function changes.

atomic arrangement, *e.g.* similar to that suggested above for the (6×1) structure. They may again consist of chains on two levels (like those in Fig. 3a), but now in the second monolayer, with an interchain spacing specified by θ. In the range of $\theta = 0.68$–0.75, the (4×1) structure coexists with the (1.47×2) structure. The transitions between (4×1), (5×1) and (2×1) seem to proceed *via* mixed-cell structures. Once these new structures are formed, they are stable against evaporation up to 900 K and no other transitions occur in the temperature range between 100 K and 900 K.

The described irreversible transitions are summarized in Figure 8. Please be aware that Figure 8 is not a phase diagram! In this diagram, the overlayer conditions were always tested at a standard temperature of 100 K. Contrary to a phase diagram, the temperatures indicated are the annealing temperatures. As again seen from this figure, annealing of coverages between 0.07 and 0.58 above 350 to 400 K always results in a more or less complete loss of extended order. Using the term "extended order" we mean both long-range and quasi-long-range order unless a commensurate or incommensurate two-dimensional crystal phase is specified.

The annealing induced structural modifications in the adsorbed films are directly coupled with changes of work function. The annealing effect on the work function is readily seen from the coverage dependences taken for LT and HT (1000 K) annealing (Fig. 9). Circles and crosses at a given coverage mark the work function changes, $\Delta\phi$, before and after HT annealing, respectively, *i.e.* the difference at fixed coverage is the annealing effect. The lines, which are just guides to the eye, underline the observed tendencies. At small coverages, $|\Delta\phi|$ is reduced upon HT annealing by some amount over a fairly wide coverage range (*i.e.* up to $\theta \approx 0.6$). Between $\theta = 0.6$ and 0.7, $\Delta\phi$ remains unchanged upon annealing, whereas for higher coverages the effect is reversed, *i.e.* $|\Delta\phi|$ increases after annealing. As seen from this figure, there is a remarkably good correlation between these variations and the structural transformations upon annealing (compare with Fig. 6). This correlation is even better seen by plotting work function data as a function of annealing temperature. This is done in Figure 10, where we plotted separately the annealing induced work function changes for various fixed coverages.

4 Discussion

The set of structures of Dy overlayers on Mo(112) found in our work before and after annealing to high temperatures is in a rather poor agreement with findings reported in the early work [5] (see Introduction). Only the c(1.56×2)structure has been observed both in reference [5] and by us, but a discrepancy exists already concerning the stability of this structure. Meanwhile experimental results have been reported for three other rare-earth adsorbates on Mo(112), namely Gd [17,18], Ho [19] and Yb [20], which qualitatively agree with our own results. An annealing effect on the film structure has been observed in all three cases, which is similar in many details to that found by us for the Dy overlayers. In particular, annealed low-coverage adlayers both of Gd and Ho show no long-range order, whereas annealed high-coverage adlayers ($\theta > 0.67$) form a series of structures similar to those formed by Dy: c(1.5×2), (4×1) and (5×1). At low temperature ($T < 300$ K), low-coverage films of Ho, Yb and even La (see note in Ref. [21]) form metastable chain structures. Therefore, the good agreement of our data with those for other rare-earth systems on Mo(112), which clearly show common trends for all of these systems, gives us confidence that our data are correct. At the moment we cannot give an obvious reason why the data reported in the early work [5] are at variance with ours.

The metastable structures of Dy on Mo(112) found below room temperature fit into the large class of adsorbate systems (mostly alkali and alkaline-earth metal atoms) investigated on this strongly anisotropic substrate [1]. They can be classified into low-coverage chain structures with close packed chains normal to the substrate troughs. These structures seem to be mostly coupled to the "ionic" range of bonding [22], evident by a strong decrease of the work function. Note, however, that indirect (*i.e.* strongly anisotropic) coupling between the adsorbed atoms through the substrate electrons plays an important role, since the simple dipole repulsion alone is not able to produce the structures observed.

The high coverage incommensurate structures with continuously variable lattice constants are formed in the "metallic" range of bonding by chains along the substrate troughs, typically above a coverage of 0.5. The peculiarity in the Dy system is, however, that chains with two atoms per unit cell seem to be formed both at low and at high coverages. This shows the adsorbate specific variability of interactions that must be mediated by the combination of valence electrons of both the adsorbate and the substrate, including the relaxations of all other electrons.

The formation of incommensurate structures already for the low coverage chain structures has also been observed for the Sr/Mo(112) system [8,4]. Here the p(8×1) structure undergoes a depinning transition close to 120 K. As mentioned above, the depinning transition in the Dy/Mo112) system may occur at temperatures lower than those available in the present system. As mentioned in Introduction, we were able to show from studies of the adsorbate induced relaxations in the Li/Mo(112) and Sr/Mo(112) systems [3,4] that a coupling mechanism by the oscillatory screening of the adsorbate induced distortion of the electron density is effective. The variability of structures seen in all these systems cannot be related to the bulk electron density at the Fermi surface, but must be due to adsorbate specific modifications of surface states. Thus the effective screening length at the surface need not be commensurate, and can induce incommensurate (or high order commensurate) structures.

For the occurrence of glass-like phases without extended order, two ingredients are important: a strong potential corrugation parallel to the surface that reduces drastically the mobility of the adatoms at a given temperature, and/or comparatively weak forces of interaction that would drive the system towards a new ordered state. Under these conditions a high temperature disordered state can easily be "frozen in" by subsequent cooling and it remains in this state. This could happen, *e.g.*, if the fraction of Dy atoms postulated to have reacted with the surface (forming a surface alloy) has a weak interaction with each other, and if it effectively blocks diffusion. Indeed there is evidence that diffusion along the troughs of the substrate in the coverage range up to 0.5 is rather slow for annealed Dy layers [23]. A diffusivity of $D = 10^{-9}$–10^{-8} cm^2/s at $T = 700$–800 K is found in reference [23]. It is lower by two orders of magnitude than that for strontium films, *e.g.*, adsorbed on the same substrate at comparable coverages [24]. The diffusion experiments for Dy on Mo(112) were carried out at temperatures which exceeded that of the irreversible transitions from metastable ordered phases (6×1) and c(1.56×2) to glass-like states. Therefore, the data of that experiment should be related to the glassy states found in our work or, perhaps, to already a very viscous liquid-like state realized at 700–800 K. The separately determined prefactors and energies of activation for diffusion of reference [23] allow us to calculate the diffusion coefficients in the temperature range $T_a = 200$–300 K optimal for ordering of the metastable (non-annealed) phases, with the result of time constants, τ_d between 10^5 and 10^3 s. This time is obviously much longer than that for the metastable phases, since considerable improvement of ordering after annealing to this temperature range has been found. Hence this fact corroborates our suggestion about the dramatic change of adatom mobility upon high-temperature annealing.

The comparison with alkali and alkaline-earth metals adsorbed on Mo(112) shows that, although substantial geometrical relaxations in the topmost substrate layers have been found in the low-coverage films [3,4], no irreversible transitions occur in these layers. This may be due to the fact that adsorbed rare-earth metals form stronger and more localized adsorption bonds since *d* and to a small extent *f* electrons are involved in bonding [1]. This stronger interaction makes exchange with substrate atoms easier, and might also deepen the substrate corrugation (possibly also even for the non-alloyed surface). This seems to be a possible reason why no long-range order was seen not only in the annealed layers of the Dy system presented here, but also in the annealed low-coverage overlayers of Gd

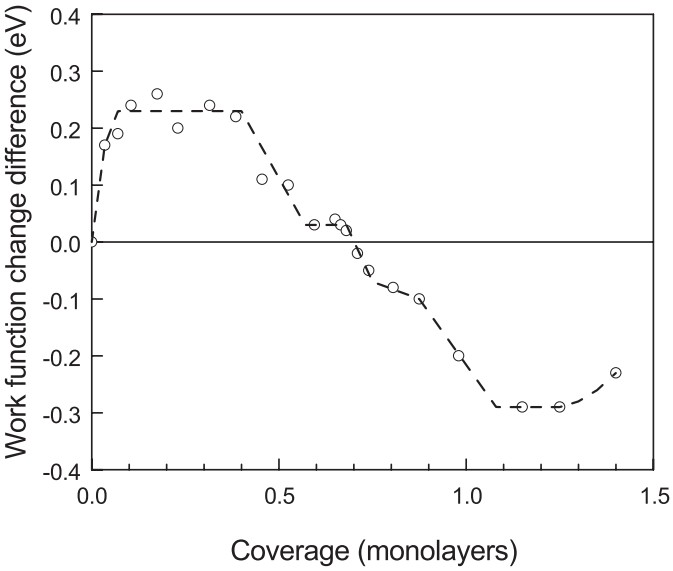

Fig. 11. Coverage dependence of the difference between the work function changes obtained after low- and high-temperature annealing. Work function is measured at T = 100 K.

and Ho on Mo(112) [18,19]. The suggestion [19,25] that this phenomenon might be due to extremely small lateral interactions caused by an adsorption induced strong reduction in the density of surface states mediating this interaction, could assist the glass formation. The partial reaction step, however, seems to be important, since without partial reaction the weakening of long-range lateral interactions would result only in a replacement of long-period chain structures by other short-period ones. Note that in the relevant case of rare-earth metal adsorption on Ta(112) with absent surface states, formation of *ordered* short-period structures upon HT annealing is found starting already at $\theta \approx 0.2$ [26].

With respect to the Dy/Mo(112) system, the observed annealing effect on the work function is fully compatible with the suggestion that the annealing driven disorder in the Dy/Mo(112) overlayers comprises an irreversible step of reaction at low coverages, which seems to reduce the adatom mobility of higher coverages. As seen in Figure 9, the $\Delta\phi$ curves for LT and HT annealing run almost in parallel at coverages below ≈ 0.5. A natural explanation of this behaviour is that upon HT annealing a small fraction of adsorbate species, $\Delta\theta$, reacts with the surface and does not contribute any more to the dipole moment of the layer. With this assumption $\Delta\theta$ is found to be 0.07. To display the $\Delta\phi$ variation caused by HT annealing at specific coverages, we plotted in Figure 11 the difference of $\Delta\phi$ before and after HT annealing as a function of coverage. This plot can be divided up into several linear segments that directly correlate with the various phases and their transitions upon annealing. The initial rising segment ends at a coverage of 0.07. Also the constant difference of 0.23 eV for coverages up to 0.4 between the $\Delta\phi$ curves before and after HT annealing corresponds to the same amount of "missing" coverage that obviously does not contribute to $\delta\phi$. In other words, the process of incorporation of Dy atoms saturates at this concentration, and only this constant amount, not a certain fraction of coverage seems to be incorporated into the first layer forming a surface alloy also at higher coverages. This first step of incorporation happens most likely at random, a precondition for the formation of the subsequent glass-like phase. The model of the chain structure suggested in Figure 3 assumes a location of half the Dy adatoms ontop of the substrate chains. Effective smoothing of such a corrugated structure during high-temperature annealing by incorporating the Dy atoms into the first substrate layer may indeed result in reduction of the negative value of work function change as found in Figure 11. Since the coverage dependence of the work function of the annealed layers in this coverage range is the same as before HT annealing – only a small fraction of coverage does not contribute –, this suggests a similar local adsorption geometry for the majority of adatoms in the annealed and non-annealed overlayers.

Above $\theta = 0.4$, $\delta\Delta\phi$ decays gradually, and almost vanishes at $\theta \approx 0.6$. The value of $\theta = 0.4$ just amounts to the sum of the Dy coverages incorporated into the surface alloy and of the completed (6×1) overlayer. The value 0.6 coincides roughly with the appearance of the stable $(n\times2)$ phases. These incommensurate phases, which seem to consist of flat layers on a single level (Fig. 3c), show very small $\delta\Delta\phi$'s in the range of their existence (coverages between 0.58 and 0.68). This is evidently a consequence of the invariance of their structure upon annealing. Since the film structure is unique here both in the non-annealed and annealed overlayer, we checked directly with LEED whether some fraction of coverage could still take part in the surface reaction during annealing. From the invariance of lattice spacing in the temperature range T_a = 100–1000 K we conclude that no reaction has occurred within an accuracy of 1% of a monolayer. Thus both work function and overlayer ordering provide evidence that the partial reaction found at lower coverage, instrumental for glass formation, is absent in this coverage range. Considering the annealing effect as a function of coverage, this means that the cause for disorder must have disappeared at $\theta \approx 0.6$. The reduction of $\delta\Delta\phi$ at coverages between 0.4 and 0.6, *i.e.* in the range of transition from "two-level" to "single-level" structures, seems to point also in this direction. It is worth noting that near $\theta \approx 0.7$, the diffusivity grows significantly forming a peak of more than two orders of magnitude [23].

The disappearance of the vitrifying transition for dense submonolayers correlates roughly with the electronic transition from the state of a local polar/covalent bond to a more delocalized metallic bond [27]. Due to direct interactions at high coverage, the adatom electrons contribute most to the formation of their own surface bands. It seems to be reasonable that adatom electrons, being involved in formation of its these bands, exert a minor effect on the substrate, so that adsorption-induced substrate corrugation may be reduced at dense coverages. A similar coverage-sensitive reconstruction phenomenon has been found for many adsorption systems [28].

At last, in the region $\theta = 0.68$–1.0, for which the annealing driven "two-level" phases are suggested to replace the "single-level" ones, an increase of $|\Delta\phi|$ by annealing was found, as expected by a higher corrugation of the adlayers. This effect is opposite to that observed for the low-coverage range ($\theta \leq 0.07$) where annealing results in smoothing the adlayer. This finding gives an additional argument for models with two-level location of Dy adatoms in the (6×1) structure (see Fig. 3a) as well as in the (5×1) and (2×1) structures, which were motivated not only by the LEED patterns and their coverage relationship, but also by the work function changes occurring concurrently with structural transitions induced by annealing.

5 Conclusions

Rare earth elements like dysprosium on strongly corrugated transition metal surfaces seem to react stronger with the surface than alkali and alkaline-earth metals. This makes the adsorbate induced structures formed at low temperature metastable.

The Dy system on Mo(112) is a particularly interesting case since both the metastable and the annealed structures can be observed and studied in detail. The both low- and high-coverage metastable structures fit into the class of systems found in adsorbed alkali and alkaline-earth metals on this and similar surfaces, although the details make the variability of possible interactions in these systems evident.

The annealing driven transition to a glass-like phase at coverages up to 0.58 seems to be coupled with partial reaction with the first substrate layer, which also changes the work function by a constant amount. It leads to a strong reduction of the diffusion coefficient in these layers so that the formation of a two-dimensional glass becomes understandable.

Interestingly, close to completion of the first adsorbed layer the annealing driven vitrifying effect vanishes, whereas at higher coverages annealing produces new ordered states. This change of behaviour is correlated with the transition from the more ionic type of adsorbate bonding to the surface to a metallic bond. This may also cause a structural change at the interface so that the adsorbed Dy atoms again form a smooth interface at these high coverages.

This work was supported by the Basic Research Foundation of the Ministry of Ukraine for Education and Science. Support by the Volkswagen-Stiftung and by the Deutsche Forschungsgemeinschaft is also gratefully acknowledged.

References

1. O.M. Braun, V.K. Medvedev, Usp. Fiz. Nauk **157**, 631 (1989); [Sov. Phys.-Usp. **32**, 328 (1989)].
2. D. Kolthoff, H. Pfnür, A.G. Fedorus, V. Koval, Surf. Sci. **439**, 234 (1999).
3. D. Kolthoff, H. Pfnür, Surf. Sci. **457**, 134 (2000).
4. D. Kolthoff, H. Pfnür, Surf. Sci. **459**, 265 (2000).
5. F.M. Gonchar, V.K. Medvedev, T.P. Smereka, G.V. Babkin, Fiz. Tverd. Tela **32**, 1872 (1990); [Sov. Phys.-Solid State **32**, 1092 (1990)].
6. D. Jürgens, G. Held, H. Pfnür, Surf. Sci. **303**, 77 (1994).
7. A. Fedorus, D. Kolthoff, V. Koval, I. Lyuksyutov, A. Naumovets, H. Pfnür, Phys. Rev. B **62**, 2852 (2000).
8. A. Fedorus, G. Godzik, V. Koval, A. Naumovets, H. Pfnür, Surf. Sci. **460**, 229 (2000).
9. I.F. Lyuksyutov, V.K. Medvedev, I.N. Yakovkin, Zh. Eksp. Teor. Fiz. **80**, 2452 (1981); [Sov. Phys.-JETP **53**, 1284 (1981)].
10. V.K. Medvedev, T.P. Smereka, Fiz. Tverd. Tela **15**, 724 (1973); [Sov. Phys.-Solid State **15**, 507 (1973)].
11. A. Fedorus, D. Kolthoff, V. Koval, I. Lyuksyutov, A. Naumovets, H. Pfnür, Europhys. Lett. **48**, 442 (1999).
12. I.F. Lyuksyutov, Zh. Eksp. Teor. Fiz. **89**, 1061 (1985); [Sov. Phys.-JETP **62**, 615 (1985)].
13. A.G. Fedorus, A.G. Naumovets, Surf. Sci. **21**, 426 (1970).
14. C.G. Shaw, S.C. Fain, M.D. Chinn, Phys. Rev. Lett. **41**, 955 (1978).
15. A.D. Novaco, J.P. McTague, Phys. Rev. Lett. **38**, 1286 (1976).
16. G.V. Uimin, L.N. Shchur, Pis'ma Zh. Eksp. Teor. Fiz. **28**, 20 (1978); [Sov. Phys.-JETP Lett. **28**, 20 (1978)].
17. C. Waldfried, D.N. McIlroy, P.A. Dowben, J. Phys. Cond. Matt. **9**, 10615 (1997).
18. Ya.B. Losovyj, Vacuum **48**, 185 (1997).
19. Ya.B. Losovyj, N.T. Dubyk, Vacuum **54**, 25 (1999).
20. I. Ubogyi, S. Stepanovskyi, J. Kolaczkiewicz, Phys. Rev. B **61**, 11097 (2000).
21. F.M. Gonchar, V.K. Medvedev, T.P. Smereka, Ya.B. Losovyj, G.V. Babkin, Fiz. Tverd. Tela **29**, 2833 (1987); [Sov. Phys.-Solid State **29**, 1629 (1987)].
22. R.D. Diehl, R. McGrath, J. Phys. C **9**, 951 (1997).
23. A.T. Loburets, A.G. Naumovets, Yu.S. Vedula, Surf. Sci. **399**, 297 (1998).
24. A.T. Loburets, N.B. Senenko, A.G. Naumovets, Yu.S. Vedula, Phys. Low-Dim. Struct. **10/11**, 49 (1995).
25. Ya.B. Losovyj, Vacuum **54**, 19 (1999).
26. V.K. Medvedev, T.P. Smereka, I.M. Ubogy, Ukr. Fiz. Zh. **40**, 344 (1995).
27. G.A. Katrich, V.V. Klimov, I.N. Yakovkin, J. Electr. Spectr. Rel. Phen. **68**, 369 (1994).
28. C.J. Barnes, in *The Chemical Physics of Solid Surfaces*, Vol. 7, edited by D.A. King, D.P. Woodruff (Elsevier, Amsterdam, 1994), p. 501.